Author Manuscript

Author Manuscript

Author Manuscript

Author Manuscript

HHS Public Access

Author manuscript

Gene. Author manuscript; available in PMC 2019 December 30.

Published in final edited form as:

Gene. 2018 December 30; 679: 219–231. doi:10.1016/j.gene.2018.09.002.

High-throughput gene expression analysis identifies p53-dependent and -independent pathways contributing to the adrenocortical dysplasia (*acd*) phenotype

Ceren Sucularli[a], **Peedikayil Thomas**[b,d], **Hande Kocak**[b,c], **James S. White**[d], **Bridget C. O'Connor**[d], and **Catherine E. Keegan**[b,d,*]

[a]Department of Bioinformatics, Institute of Health Sciences, Hacettepe University, 06100, Ankara, TURKEY

[b]Department of Human Genetics, University of Michigan, Ann Arbor, Michigan, USA

[c]Department of Medical Biology and Genetics, Istanbul Bilim University, Istanbul, TURKEY

[d]Department of Pediatrics, University of Michigan, Ann Arbor, Michigan, USA

Abstract

In mammalian cells TPP1, encoded by the *Acd* gene, is a key component of the Shelterin complex, which is required for telomere length maintenance and telomere protection. In mice, a hypomorphic mutation in *Acd* causes the adrenocortical dysplasia (*acd*) phenotype, which includes limb and body axis anomalies, and perinatal lethality. p53 deficiency partially rescues limb and body axis anomalies in *acd* mutant embryos, but not perinatal lethality, implicating p53-independent mechanisms in the *acd* phenotype. Loss of function of most shelterin proteins results in early embryonic lethality. Thus, study of the hypomorphic *acd* allele provides a unique opportunity to understand telomere dysfunction at an organismal level. The aim of this study was to identify transcriptome alterations in *acd* mutant and *acd, p53* double mutant embryos to

[*]**Corresponding author:** Catherine Keegan, MD, PhD, Department of Pediatrics, Division of Genetics, Department of Human Genetics, 8220A MSRB III, SPC 5646, 1150 W. Medical Center Dr. Ann Arbor, MI 48109, keeganc@med.umich.edu.

Conflicts of interest

Ceren Sucularli declares that she has no conflicts of interest. Peedikayil Thomas declares that he has no conflicts of interest. Hande Kocak declares that she has no conflicts of interest. James White declares that he has no conflicts of interest. Bridget O'Connor declares that she has no conflicts of interest. Catherine Keegan declares that she has no conflicts of interest.

Ethical Approval

All applicable international, national, and/or institutional guidelines for the care and use of animals were followed. This article does not contain any studies with human participants performed by any of the authors.

Data availability

The microarray data are publicly available in the GEO repository under accession number GSE95806 (*GEO: GSE95806*).

CRediT Author Statement:

Ceren Sucularli: Methodology, Validation, Formal Analysis, Investigation, Writing - Original Draft, Writing - Review and Editing, Visualization. **Peedikayil Thomas**: Validation, Formal Analysis, Investigation, Writing – Review and Editing. **Hande Kocak**: Validation, Formal Analysis, Investigation, Writing – Review and Editing. **James S. White**: Validation, Formal Analysis, Investigation. **Bridget C. O'Connor**: Validation, Formal Analysis, Investigation. **Catherine E. Keegan**: Conceptualization, Validation, Resources, Writing – Review and Editing, Supervision, Project Administration, Funding Acquisition

Publisher's Disclaimer: This is a PDF file of an unedited manuscript that has been accepted for publication. As a service to our customers we are providing this early version of the manuscript. The manuscript will undergo copyediting, typesetting, and review of the resulting proof before it is published in its final citable form. Please note that during the production process errors may be discovered which could affect the content, and all legal disclaimers that apply to the journal pertain.

Author Manuscript Author Manuscript Author Manuscript Author Manuscript

understand the p53-dependent and –independent factors that contribute to the mutant phenotypes in the context of the whole organism. Genes involved in developmental processes, cell cycle, metabolic pathways, tight junctions, axon guidance and signaling pathways were regulated by p53-driven mechanisms in *acd* mutant embryos, while genes functioning in immune response, and RNA processing were altered independently of p53 in *acd*, *p53* double mutant embryos. To our best of knowledge, this is the first study revealing detailed transcriptomic alterations, reflecting novel p53-dependent and –independent pathways contributing to the *acd* phenotype. Our data confirm the importance of cell cycle and DNA repair pathways, and suggest novel links between telomere dysfunction and immune system regulation and the splicing machinery. Given the broad applicability of telomere maintenance in growth, development, and genome stability, our data will also provide a rich resource for others studying telomere maintenance and DNA damage responses in mammalian model systems.

Keywords

Gene expression; Microarray; Mouse model of disease; p53; Pathway analysis; Shelterin complex

1. Introduction

In eukaryotic cells, telomeres are structures responsible for the protection of chromosome ends. Telomeres consist of repetitive DNA sequences including both double-stranded repeats and a single-stranded 3’ overhang (Palm and de Lange, 2008). In mammalian cells, the shelterin complex binds to telomeres and serves two important roles: protection of telomere ends and maintenance of telomere length (Palm and de Lange, 2008). Disrupted function of the shelterin complex results in telomere deprotection, which initiates a DNA damage response followed by induction of apoptosis or senescence (Karlseder et al., 1999). In humans, germline mutations in shelterin complex proteins have been associated with inherited bone marrow failure syndromes, such as dyskeratosis congenita (DC) (Savage et al., 2008; Walne et al., 2008) and Hoyeraal-Hreidarsson syndrome (HHS) (Kocak et al., 2014). Germline and somatic mutations in shelterin proteins have been associated with multiple types of cancer, including melanoma, leukemia, and glioma (Jones et al., 2016). In mouse, knockout of the majority of genes encoding shelterin proteins exhibit early embryonic lethality (Karlseder et al., 2003; Chiang et al., 2004; Celli and de Lange, 2005; Hockemeyer et al., 2006; Wu et al., 2006). Although numerous studies have been performed with cell lines that carry mutations in shelterin complex genes to further the understanding of their cellular and biochemical functions (reviewed in (Jones et al., 2016), these studies lack the ability to understand the phenotypes resulting from telomere dysfunction at the organismal level, which likely have relevance for the human syndromes and cancer phenotypes. To fill this gap in knowledge, we undertook detailed transciptome studies to begin to decipher the underlying mechanisms leading to the organismal phenotypes caused by disruptions in the shelterin complex, with the goal of laying the groundwork for further functional and experimental research.

The shelterin complex is comprised of six proteins, TRF1 (Telomere repeat factor-1), TRF2 (Telomere repeat factor-2), POT1 (protection of telomeres-1), RAP1 (the human homolog of

Author Manuscript Author Manuscript Author Manuscript Author Manuscript

the yeast telomeric protein Rap1), TIN2 (TRF1- interacting protein 2) and TPP1. Shelterin proteins, separately or in combination, protect chromosome ends from being recognized as double stranded breaks by the DNA repair machinery (Guo et al., 2007; Sfeir and de Lange, 2012). Among the six proteins, TRF1 and TRF2 bind double stranded telomere repeats, while POT1 binds to the single stranded 3' overhang (Broccoli et al., 1997; Baumann and Cech, 2001). TRF1 and TRF2 function in maintaining telomere length (Smogorzewska et al., 2000). TRF1 is also essential for replication of telomeric DNA (Sfeir et al., 2009). RAP1, which is recruited to telomeres by TRF2, functions in telomere length and gene expression regulation (Li and de Lange, 2003; O'Connor et al., 2004; Martinez et al., 2010). TIN2 is a bridging protein that connects TRF1 and TRF2 to TPP1 and is involved in recruitment of TPP1/POT1 to telomeres (Houghtaling et al., 2004; Liu et al., 2004; Ye et al., 2004; Takai et al., 2011).

TPP1, encoded by the *Acd* gene, is highly important in telomere length maintenance; the TPP1/POT1 heterodimer contributes to telomere elongation by recruiting telomerase to telomeres and increasing the processivity of telomerase (Wang et al., 2007; Xin et al., 2007; Latrick and Cech, 2010). In addition to telomere elongation, TPP1 is crucial for telomere end-protection (Kibe et al., 2010). TPP1 also increases the affinity of POT1 for single stranded telomeric DNA (Wang et al., 2007; Xin et al., 2007).

In the mouse, the adrenocortical dysplasia ($Acd^{acd/acd}$, hereafter referred to as *acd* mutant) phenotype originated from a spontaneous autosomal recessive splice site mutation in the *Acd* gene. Homozygous *acd* mutant mice were first described because of their abnormal adrenal gland appearance (Beamer et al., 1994). Further characterization of the mutant phenotype revealed striking pleiotropy and background strain dependence (Keegan et al., 2005). On the DW/J and C57BL6/J strains, the *acd* mutation causes perinatal lethality, caudal truncation, and limb and vertebral segmentation defects, similar to phenotypes observed in human Caudal Regression syndrome (CRS) and VACTERL association. On the CAST/Ei background strain, homozygous *acd* mutant mice survive with a phenotype characterized by severe growth retardation, hyperpigmentation, and infertility. While these strain-specific differences are striking, it is likely that the underlying cellular mechanisms contributing to the phenotypes are similar. Therefore, our comprehensive gene expression analysis during mouse embryogenesis is an excellent model for understanding the cellular pathways that contribute to the organismal phenotypes.

Previous studies demonstrated that p53-dependent apoptosis resulting from telomere dysfunction is the cause of the caudal regression phenotype in *acd* mutant embryos (Vlangos et al., 2009). On the C57BL6/J background, p53 deficiency rescues many features of caudal regression, but not the perinatal lethality, and although the limb hypoplasia is rescued, double mutant embryos still exhibit polydactyly. On a mixed CAST/Ei background, p53 deficiency results in a partial rescue of the *acd* phenotype but also causes an increase in tumorigenesis (Else et al., 2009). Complete deficiency of *Acd* is lethal early in development; thus, the spontaneous *acd* mutation is a hypomorphic allele (Kibe et al., 2010). Deficiency of *Acd* in the bone marrow leads to rapid depletion of hematopoietic stem cells, which is not rescued by p53 deficiency (Jones et al., 2014). Consequently, there may be p53-independent mechanisms in double mutant mice that are critical for specific aspects of the *acd* mutant

Author Manuscript Author Manuscript Author Manuscript Author Manuscript

phenotype, including the perinatal lethality. In this study, we performed gene expression profiling to identify differentially expressed genes in *acd* mutant and *acd*, *p53* double mutant embryos when compared to wild type embryos to fully understand those phenotypes at the molecular level. We aimed to characterize p53-dependent and – independent pathways contributing to the *acd* mutant phenotype with the goal of improving our understanding of diseases related to dysfunctional telomeres and contributing to a search for new therapeutic approaches to conditions characterized by telomere dysfunction. Expression of genes in cell cycle, metabolic pathways, and signaling pathways were regulated in a p53-dependent manner. Expression of immune system and related pathways, and RNA processing genes were altered in the setting of p53 deficiency and therefore independent of *p53* expression. Microarray results were confirmed with RT-qPCR and a significant correlation between the microarray and RTqPCR data was observed. Our study provides detailed gene expression profiles of *acd* and double mutant embryos, and reveals the altered molecular mechanisms in response to *p53* expression or deficiency.

2. Material and methods

2.1. Animals

Sources of adrenocortical dysplasia (Acd^{acd}) and $p53^{-/-}$ mice were previously described (Vlangos et al., 2009). Both mutant strains were maintained on a C57BL6/J background. Mice were housed in specific pathogen free and environmentally controlled conditions with 14 hour light/10 hour dark cycles. Food and water were provided *ad libitum*. All experiments involving mice were approved by The University of Michigan Institutional Animal Care and Use Committee (IACUC).

2.2. Timed pregnancies

Matings between male and female *acd/+*, $p53^{+/-}$ mice for timed pregnancies were set up using standard animal husbandry techniques. Noon on the day that a vaginal plug was observed was considered E0.5. Embryos were genotyped using DNA isolated from yolk sac as previously described (Keegan et al., 2005).

2.3. RNA isolation

RNA from whole embryos was isolated with Qiagen RNeasy® Mini Kit (74104, Qiagen, Valencia, CA, USA) according to the manufacturer's instructions. Homogenization of embryos was performed with a Polytron homogenizer in RLT lysis buffer. On-column DNA digestion was performed by using RNase-Free DNase Set (79254, Qiagen, Valencia, CA, USA). RNA quality and quantity were checked using a NanoDrop 2000.

2.4. Microarray data analysis

High-throughput microarray analysis was performed with Affymetrix GeneChip Mouse Genome 430 2.0 Array (Affymetrix, Santa Clara, CA, USA). Whole embryo RNA was isolated from wild type (wt), *acd* mutant ($Acd^{acd/acd}$), $p53^{-/-}$, and double mutant ($Acd^{acd/acd}$, $p53^{-/-}$) embryos (n=3 from each group) at E10.5 and hybridized onto array chips according to manufacturer's instructions (Affymetrix, Santa Clara, CA, USA). Quality control of the arrays and RNA integrity were performed by using *affy* (Gautier et al., 2004) and *affyPLM*

Author Manuscript Author Manuscript Author Manuscript Author Manuscript

(Bolstad BM, 2005) packages in R software, version 3.0.2 (https://www.r-project.org) (Figs. S1 and S2). CEL files were normalized using justRMA algorithm and differentially expressed genes, according to pair-wise comparisons, were selected using BRB-Array tools version 4.4.0 (http://linus.ncbi.nih.gov/BRB-ArrayTools.html; developed by Dr. Richard Simon and the BRBArrayTools Development Team). Bioconductor (www.bioconductor.org) annotation package mouse4302.db (version 3.0.0) was used for annotation of probe sets to related gene names along with gene information by BRB-Array tools version 4.4.0. Data was submitted to the Gene Expression Omnibus (GEO) repository (https://www.ncbi.nlm.nih.gov/geo/) with accession number GSE95806 (*GEO: GSE95806*).

2.5. Identification of differentially expressed probe sets

For the selection of differentially expressed probe sets and related genes, the Class Comparison Function of BRB-Array Tools was used. Probe sets with $p < 0.05$ significance threshold for the univariate test were selected as differentially expressed. Genes contributing to the *acd* phenotype dependent upon p53 and genes independent of p53 were identified by determining differentially expressed probe sets between double mutant and *acd* embryos.

2.6. Heat-maps of differentially expressed probe sets

Heat-maps of differentially expressed probe sets were prepared by hierarchically clustering probe sets and arrays according to Euclidian distance similarity metric and average linkage clustering with Cluster 3.0 (Eisen et al., 1998; de Hoon et al., 2004). Heat-maps were visualized with Java Treeview version 1.1.6r4 (Saldanha, 2004).

2.7. Gene Ontology (GO) terms for Biological Process (BP) and KEGG pathway annotations of probe sets

Functional annotation of differentially expressed genes to GO terms BP and KEGG pathway terms was performed using DAVID 6.7 (Huang da et al., 2009b; Huang da et al., 2009a). The threshold EASE (p-value) was set to 0.05 for obtaining significant KEGG and BP terms. Significant GO terms are shown in supplemental Tables S1-S8.

2.8. RT-qPCR validation

Three μg DNA free total RNA with RIN values >9.9 were reverse transcribed using Invitrogen SuperScript IV first strand synthesis system according to the manufacturer's instructions. Three RNA samples from each group were reverse transcribed independently and simultaneously. qPCR for each cDNA product was performed in triplicate. Applied Biosystems SYBR Green PCR Master Mix and StepOnePlus Real-Time PCR system were used for qPCR. Initial denaturation was done at 95°C for 10 min, annealing and extension at 60°C for 60 sec with subsequent denaturation at 95°C for 15 sec for 40 cycles, followed by instrument default melt curve analysis. PCR yielded single specific band for each reaction as predicted by the programs. Primers spanning an intron were designed to yield single specific RT-qPCR product between 100–200 bp using Primer3 from UCSC Genome Browser on mouse July 2007 (NCBI137/mm9) assembly (Table S9). The equation $2^{-\Delta\Delta Ct}$ was used to calculate fold expression change of selected genes (Livak and Schmittgen, 2001). The Log_2 transformed fold change values were used for graphs and all statistical analyses.

Author Manuscript Author Manuscript Author Manuscript Author Manuscript

2.9. Statistical analysis of RT-qPCR

The statistical significance between groups (wt, *p53*$^{-/-}$, *acd* mutant and double mutant) was evaluated with one-way analysis of variance (ANOVA) with Tukey multiple comparison test. The Pearson correlation coefficient and related P-value were calculated between microarray and RT-qPCR results for *acd* vs. wt and double mutant vs. wt comparisons, separately. P<0.05 was considered to be statistically significant. All statistical analyses for RT-qPCR were performed using IBM SPSS Statistics Version 23.0 (IBM Corp., Armonk, NY, USA). The RT-qPCR graphs were generated using GraphPad Prism version 7.0d for Mac Trial version (GraphPad Software, La Jolla, CA, USA, www.graphpad.com).

3. Results

3.1. The effect of Acd deficiency on gene expression in acd mutant embryos

3344 probe sets (1616 up, 1728 down) among the ≈45000 probe sets on the array chips were identified as significantly changed between *acd* mutant and wt embryos (p<0.05, Fig. 1A). The *Acd* gene is represented by a single probe set in the Affymetrix GeneChip Mouse Genome 430 2.0 Array, according to BRB-Array tools version 4.4.0 annotation. As expected, this probe set (1420882_a_at) showed significant down-regulation ($p=8\times10^{-7}$) in *acd* mutant embryos.

To determine which pathways were significantly dysregulated in *acd* mutant embryos, KEGG pathway and GO annotations for BP of significantly upregulated and downregulated probe sets were performed with DAVID functional annotation tool. Upregulated genes in *acd* embryos clustered in three main categories; cancer related pathways/cell cycle, immune system related pathways and junction/adhesion (Fig. 1B, Table S1), while downregulated genes clustered in axon guidance, regulation of transcription, development, morphogenesis, and differentiation, and components of signaling pathways, including MAPK, ErbB, Wnt, and insulin signaling pathways (Fig. 1C, Table S2).

3.2. The effect of combined Acd and p53 deficiency on gene expression in double mutant embryos

Next, we asked which pathways were dysregulated in double mutant embryos (*acd/acd p53*$^{-/-}$), carrying a null allele of *p53* in addition to the *acd* mutant allele (Jacks et al., 1994). When we compared gene expression profiles of double mutant and wt embryos, 2023 probe sets (1046 upregulated and 977 downregulated) showed significant differential expression (p<0.05, Fig. 2A). One double mutant sample clustered closely to two wt samples, likely because they were littermates. As expected, the probe set representing *Acd* was significantly downregulated in double mutant embryos ($p=1.6\times10^{-4}$). The *Trp53* gene is represented by 6 probe sets in the Affymetrix GeneChip Mouse Genome 430 2.0 Array, (according to BRB-ArrayTools version 4.4.0, Bioconductor (www.bioconductor.org) annotation package mouse4302.db, version 3.0.0), which are 1426538_a_at, 1427739_a_at, 1438808_at, 1457623_x_at, 1459780_at, 1459781_x_at). Of the six probe sets, four showed significant changes in double mutant embryos; 1438808_at was upregulated (p=0.012) and 1426538_a_at ($p=8.75\times10^{-5}$), 1427739_a_at (p=0.0003), 1457623_x_at (p=0.007) were downregulated. We searched probe set IDs in the Affymetrix database (https://

Author Manuscript Author Manuscript Author Manuscript Author Manuscript

www.affymetrix.com/analysis/index.affx) and confirmed that all probe sets represent the *Trp53* gene. We found probe set sequences in the Affymetrix database (https://www.affymetrix.com/analysis/index.affx) and BLAST searched the sequence against the mouse genome (GRCm38) in the ENSEMBL database (http://www.ensembl.org/).Of the downregulated probe sets, two were in exons of *Trp53* and one was located in the 3'UTR. The other three probe sets, which were either upregulated or not significantly changed, were intronic (Figure S3).

Immune response was detected as a significant KEGG pathway and GO-BP term for upregulated genes in double mutant embryos (Fig. 2B, Table S3), while RNA processing and transcription regulation were significant KEGG pathway and GO-BP terms for downregulated genes (Fig. 2C, Table S4).

Some genes within the p53 signaling pathway were either upregulated or downregulated in double mutant embryos, resulting in appearance of p53 signaling pathway in both upregulated and downregulated KEGG pathway lists (Fig. 2B and Fig. 2C). In addition to *Trp53*, some genes that are known to be transcriptional targets of p53 protein and involved in apoptotic response and DNA damage were detected in the downregulated gene list, such as *Bbc3* (*BCL2 binding component 3*, also known as *Puma*) (Nakano and Vousden, 2001), *Pten* (*phosphatase and tensin homolog*) (Stambolic et al., 2001) and *Ccng1* (*cyclin G1*) (Kimura et al., 2001). The upregulated genes within the p53 signaling pathway were involved in cell death, such as *Casp3* (*caspase 3*), *Ddb2* (*damage specific DNA binding protein 2*) and *Gadd45b* (*growth arrest and DNA-damage-inducible 45 beta*). Notably, it has been shown that both *Ddb2* and *Gadd45b* expression are not responsive to P53 in mouse (Vairapandi et al., 1996; Tan and Chu, 2002).

3.3. Identification of p53-dependent and –independent pathways contributing to the acd mutant phenotype

To identify gene sets contributing to formation of the *acd* phenotype that are dependent on expression of p53 and gene sets whose expression was changed independently of *p53*, we performed serial comparisons and eliminations. First, the effect of *p53* deficiency alone on gene expression was determined by comparing the probe sets in *p53* mutant to wt embryos. Probe sets that were differentially expressed in response to *p53* deficiency were identified ($p<0.05$, 808 upregulated probe sets and 681 downregulated probe sets). Overlapping probe sets (61 upregulated and 77 downregulated) between *p53* mutant and double mutant embryos were then excluded from the list of significant probe sets of double mutant embryos (Fig. 3A). From that point, all comparisons involving double mutant embryos were performed with the remaining probe sets (985 up and 900 down) after the exclusion of probes changing due to p53 deficiency (Fig. 3B).

To understand the effect of p53 deficiency on gene expression in *acd* embryos, the significantly changed probe sets in double mutant vs. wt embryos (985 up and 900 down) and *acd* mutant vs. wt embryos (1616 up and 1728 down) were compared. p53-dependent pathways contributing to the formation of the *acd* phenotype were identified by finding the significantly changing probe sets only in *acd* mutant (compared to wt) embryos (which are $p53^{+/+}$), but not in double mutant embryos (compared to wt) (Fig. 3B). In order to find the

Author Manuscript Author Manuscript Author Manuscript Author Manuscript

probe sets that were significantly changed when *p53* is absent, therefore regulated by *p53*-independent mechanisms, the differentially expressed probe sets of double mutant vs. wt (985 up and 900 down) and *acd* mutant vs. wt (1616 up and 1728 down) embryos were compared, and the probe sets that were changed in double mutant (compared to wt) embryos but not in *acd* mutant embryos (compared to wt) were identified (Fig. 3B). Of the 1616 upregulated and 1728 downregulated probe sets in *acd* mutant embryos (Fig. 1A), 1411 probe sets were upregulated and 1627 probe sets were downregulated only in *acd* mutant embryos, while 205 upregulated and 101 downregulated probe sets were shared between *acd* and double mutant embryos, representing genes that are responsive to the *acd* mutation but do not depend on expression of *p53* (Fig. 3B). According to our comparison, expression of 1411 upregulated and 1627 downregulated probe sets did not show a significant change in double mutant embryos; therefore, we concluded that expression of these genes (1411 up and 1627 down) was responsive to p53 in *acd* mutants. 780 upregulated and 799 downregulated probe sets were detected as significantly changed only in double mutant embryos; thus, expression of these probe sets was altered independent of p53 expression (Fig. 3B).

3.4. Functional annotation of p53–dependent probe sets involved in the acd phenotype

Functional annotation of 1411 upregulated and 1627 downregulated probe sets that were significantly changed in only in *acd* mutant embryos, therefore dependent upon p53, was performed by using DAVID functional annotation tool. Genes involved in cell cycle, metabolic pathways, and tight junctions were found to be upregulated (Fig. 4A, Table S5). We observed upregulation of p53 signaling pathway members *Trp53*, *Ccnd1* (Cyclin D1), *Cdkn1a* (*p21*, Cyclin-Dependent Kinase Inhibitor 1A), which also appeared in terms for cell cycle and cellular response to stress, in *acd* mutant embryos. Although some cell division genes, such as *Cyclin D2* and *Cyclin E1*, were increased, expression of several members of signaling pathways involved in transcription and development were decreased in *acd* mutant embryos. Genes involved in the ErbB, MAPK, Wnt, GnRH, VEGF and Jak-STAT signaling pathways and axon guidance showed a significant decrease (Fig. 4B, Table S6).

Genes involved in cancer related pathways changed in opposite directions; the term “mmu05200: Pathways in cancer” appeared in both upregulated and downregulated KEGG pathway lists (Fig. 4A and Fig. 4B). Since this is a broad term encompassing several signaling mechanisms with many activator and repressor proteins, it is not surprising that some components were upregulated and some were downregulated.

3.5. Functional annotation of p53–independent probe sets involved in the acd phenotype

1579 probe sets (780 up and 799 down) were significantly changed only in double mutant embryos (Fig. 3B) and not in *acd* mutant embryos, representing the genes regulated independently of p53. Functional annotation was performed to find the genes and pathways that belong to those probe sets. Genes involved in the immune response and related pathways were significantly increased in double mutant embryos (Fig. 5A, Table S7). Several chemokine ligands (*CCL4*, *CCL6*, *CCL8*, *CCL25, CXCL14,* and *CXCL12*) were observed in the upregulated immune response genes. Genes involved in RNA processing, ubiquitin mediated proteolysis, mTOR signaling, phosphatidyl inositol signaling, regulation

Author Manuscript Author Manuscript Author Manuscript Author Manuscript

of transcription and cell cycle were significantly decreased in double mutant embryos (Fig. 5B, Table S8). Expression of DNA repair genes responded differently to p53 deficiency. Genes functioning in DNA repair, such as *Ddb2* and *Gadd45b*, were increased, while other DNA repair genes, such as *Rad21* and *Bard1* (BRCA1 associated RING domain 1), were decreased in double mutant embryos.

3.6. Functional annotation of shared genes between acd mutant and double mutant embryos

According to functional annotation of the 205 upregulated and 101 downregulated probe sets that were significantly changed in both *acd* and double mutant embryos, genes involved in immune response and related pathways, and cell death, such as *XIAP* (X-linked inhibitor of apoptosis) and *Casp3*, were upregulated (Fig. 6A and Fig. 7A), and genes involved in axon guidance, transcriptional regulation, limb morphogenesis and development were significantly decreased in both *acd* mutant and double mutant embryos (Fig. 6B and Fig. 7B).

3.7. Validation of microarray results with RT-qPCR

Eight genes functioning in immune response, spliceosome, and DNA repair that were differentially expressed in *acd* and/or double mutant embryos were selected to confirm microarray results (Fig. 8A-H). In the microarray analysis, *Prpf19*, a spliceosome component, was downregulated only in double mutant embryos, which was confirmed with RT-qPCR (Fig. 8A). *Elmo3*, an engulfment factor, was upregulated in both *acd* and double mutant embryos in the microarray, which was confirmed for both groups with RT-qPCR (Fig. 8C). *Usp18*, *Ifit1*, and *Irgm1* all function in immune response. In the microarray, *Usp18* was significantly upregulated in both *acd* and double mutant embryos, while *Ifit1* was only upregulated in double mutant embryos. We confirmed upregulation of *Usp18* and *Ifit1* in double mutant embryos with RT-qPCR (Fig. 8B and Fig. 8D). *Irgm1*, which was upregulated only in double mutant embryos, was also validated with RT-qPCR (Fig. 8E). Although similar trends to the microarray data were observed by RT-qPCR for *Cdkn1a* (p21), the splicing factor *Srsf6,* and the chemokine ligand *Cxcl14*, we did not achieve statistical significance for these genes. We did observe a significant correlation between microarray and RT-PCR data for both *acd* vs wt (Pearson's correlation coefficient=0.823, p=0.012) and double mutant vs wt (Pearson's correlation coefficient=0.891, p=0.003) comparisons.

4. Discussion

In this study, we examined the transcriptomic changes in *acd* mutant and *acd*, *p53* double mutant (*acd/acd*, $p53^{-/-}$) embryos to dissect the molecular mechanisms contributing to phenotypes resulting from telomere dysfunction *in vivo*. We also wanted to gain insight into the effect of *p53* deficiency on the *acd* phenotype by comparing gene expression profiles of *acd* mutant and *acd*, *p53* double mutant embryos. We chose whole embryo RNA for our analysis because of the ubiquitous cellular function of TPP1 in telomere maintenance during development and our previous finding of widespread apoptosis in *acd* mutant embryos at this timepoint (E10.5), which was rescued by p53 deficiency (Vlangos et al., 2009).

Author Manuscript Author Manuscript Author Manuscript Author Manuscript

The *acd* embryonic phenotype is characterized by limb and body axis anomalies with perinatal lethality in *acd* mutant embryos (Beamer et al., 1994; Keegan et al., 2005). The *acd* mutation is caused by a single nucleotide variant, resulting in disruption of a splice donor consensus site following the third exon of the *Acd* gene. Because a small amount of wild type mRNA is produced, the mutation is functionally hypomorphic and causes a mild telomere end-protection defect, including telomere dysfunction-induced foci (TIFs), anaphase bridges, telomere fusions, and radial formations (Else et al., 2007; Hockemeyer et al., 2007). According to our microarray results, the *Acd* gene was significantly downregulated ($p=8\times10^{-7}$) in *acd* embryos. The downregulation of *Acd* expression in *acd* mutant embryos is consistent with the profound deficiency of Tpp1 protein observed in *acd* mutant cells (Keegan et al., 2005; Else et al., 2007; Hockemeyer et al., 2007). Because the *Acd* splicing mutation results in aberrant transcripts with an altered reading frame and premature translation termination, the significant reduction in *Acd* expression likely reflects nonsense-mediated decay (Keegan et al., 2005; Brogna and Wen, 2009; Jones et al., 2014).

Telomere dysfunction followed by p53-dependent apoptosis during embryogenesis was observed in *acd* mutant embryos (Else et al., 2007; Vlangos et al., 2009; Jones et al., 2014). Induction of apoptosis and subsequent cell death resulting from TPP1 mutation along with telomerase inhibitor treatment was also reported in human HeLa cells (Nakashima et al., 2013). In our transcriptome analysis, we found that genes functioning in the p53-signaling pathway (Fig. 1B and Fig. 4A), including *Cyclin D1*, *Cyclin D2*, *Fas*, *Cdkn1a* (*p21*) and *Trp53*, were significantly upregulated in *acd* mutant embryos (data not shown). Several genes in this list, such as *Trp53*, *Cdkn1a* (*p21*) and *Fas*, encode important regulators of apoptosis and favor cell death (Woo et al., 1999), consistent with our previous findings demonstrating p53-dependent apoptosis in *acd* mutant embryos (Vlangos et al., 2009). We also previously showed upregulation of p21 in *Acd*-deficient hematopoietic stem cells (Jones et al., 2014). Additionally, we found that some of the cyclin genes were upregulated in *acd* mutant embryos but not in double mutant embryos. Although cyclin proteins have important roles in progression of the cell cycle and favor cell proliferation, increased expression of Cyclin D1 has been shown to induce DNA damage response (DDR) in cells (Li et al., 2010; Casimiro et al., 2012).

In addition to the p53-signaling pathway, components of several cancer related pathways, such as melanoma, prostate cancer, pathways in cancer, and cell cycle were significantly upregulated in *acd* mutant embryos (Fig. 1B and Fig. 4A). This is likely due to the fact that genes functioning in the p53-signaling pathway, such as *Cyclin D1* and *Trp53*, also function in these cancer-related pathways according to our KEGG pathway annotation results (data not shown). Interestingly, mutations in *ACD* have been identified in familial melanoma in humans (Aoude et al., 2015). In addition to those genes, fibroblast growth factor genes (*Fgf3*, *Fgf4*, *Fgf13* and *Fgf10*) and Janus kinase 1 (*Jak1*), which are related to cancer in the KEGG pathway analysis, showed increased expression in *acd* embryos (Fig. 1B and Fig. 4A). In addition to their involvement in cancer, a major role of FGF proteins is in the specification and patterning of the axes of the embryo (Dorey and Amaya, 2010), which is more likely to be relevant for our analysis in *acd* mutant mouse embryos.

Author Manuscript Author Manuscript Author Manuscript Author Manuscript

As we have previously shown, *acd* mutant embryos have disrupted axial skeletal development (Keegan et al., 2005; Vlangos et al., 2009). We detected the downregulation of multiple developmental signaling pathways, such as ErbB, MAPK, Wnt and Jak-STAT pathways, only in *acd* mutant embryos (Fig. 4B), and GO annotations showed significant downregulation of multiple developmental processes, including embryonic skeletal system development (Table S2 and Table S6), consistent with the *acd* mutant phenotype. Importantly, telomerase modulates Wnt signaling, and the Wnt signaling component ß-catenin regulates expression of the telomerase subunit *Tert*, demonstrating a critical role for Wnt signaling in telomere maintenance (Park et al., 2009; Hoffmeyer et al., 2012).

Previously, the effect of shelterin protein Rap1 deficiency (encoded by the *Terf2ip* gene) was studied in mouse embryonic fibroblast (MEF) cells (Martinez et al., 2010). Rap1 deficiency resulted in downregulation of genes functioning in cell adhesion and metabolism, insulin secretion, PPAR signaling, and growth hormone pathways, while the genes involved in ABC transporters and Type II Diabetes were upregulated in Rap1-deficient MEF cells (Martinez et al., 2010). In our microarray analysis, we observed a similar pattern of downregulated pathways; genes involved in axon guidance, insulin signaling and several signal transduction pathways were downregulated in both *acd* and double mutant embryos (Fig. 4B, Fig. 5B and Fig. 6B), which might indicate a conserved response in mouse cells to dysregulation of telomere protection -dependent or –independent of p53. Downregulation of genes involved in the insulin signaling pathway in *acd* and double mutant embryos might be related to telomere biology, since *Terc* deficient mice also showed altered glucose metabolism and insulin secretion (Kuhlow et al., 2010). In *acd* mutant mice, we observed the upregulation of genes involved in cardiomyopathy (Fig. 4A). It has been shown that telomere dysfunction induces heart pathologies in mice, including cardiomyopathy, and p53 deficiency partially rescues the heart pathophysiology induced by telomere dysfunction (Sahin et al., 2011).

We specifically examined expression of other genes within the shelterin complex or genes known to be important for telomere maintenance and did not find any significant changes in double mutant embryos. In *acd* mutant embryos, only one of the three probe sets representing Trf1 was slightly upregulated (encoded by *Terf1*, probe set 1431332_a_at, p=0.005, log2 FC=0.275), and in *p53* mutant embryos, expression of one of the four probe sets for *Pot1a* was slightly increased (probe set 1456369_at, p=0.048, log2 FC=0.239). This might suggest that these genes are regulated independently of *Acd* and *p53*. However, it should be noted that in chronic lymphocytic leukemia patients, *TP53* disruption was associated with downregulation of shelterin gene expression, although low expression of *POT1*, *TPP1* and *TIN2* was also observed in some patients with wild type *TP53* (Guieze et al., 2016). In isogenic human colon adenocarcinoma cell lines with *TP53* mutations, shelterin genes showed upregulation (*ACD/TPP1*), downregulation (*TERF1*, *POT1*, *TERF2IP*) and also normal expression (*TERF2*, *TIN2*) (Samassekou et al., 2014). These conflicting data could be due to species-specific differences in shelterin gene expression in response to p53 deficiency. It is also possible that regulation of shelterin gene expression is more complex and regulated by multiple factors.

Since only a limited number of probe sets were shared between *acd* and double mutant embryos (Fig. 3B, 205 upregulated and 101 downregulated), we observed a high degree of

Author Manuscript Author Manuscript Author Manuscript Author Manuscript

similarity in the KEGG pathway results in Fig. 1 and Fig. 4, and BP results in Tables S1-S2 and Tables S5-S6. This might also indicate that the majority of genes significantly changing in *acd* mutant embryos are p53-dependent.

To define p53-independent pathways, we examined genes that were up- or downregulated in the setting of *p53* deficiency. We have previously shown that *p53* deficiency rescues the limb hypoplasia and vertebral abnormalities but not the perinatal lethality in double mutant mice (Vlangos et. al., 2009). In addition, although the limb hypoplasia phenotype is rescued, double mutant mice display polydactyly, indicating persistent dysregulation of limb development. Consistent with the partially rescued phenotype, we observed downregulation of a limited number of genes functioning in proximal/distal pattern formation, limb development and morphogenesis in both *acd* and double mutant embryos (Fig. 7B). However, some GO BP terms for development, morphogenesis, and differentiation that were downregulated in *acd* mutant embryos were upregulated in double mutant embryos (Compare Table S6 to Table S7). In addition, genes functioning in bone development were increased in double mutant embryos, along with genes for other developmental processes, such as neuron and forebrain development (Table S7), suggesting p53-independent mechanisms. According to our BP annotations, some nervous system genes were responsive to *p53* deficiency; in double mutant embryos, we observed upregulation of neuronal development and differentiation genes (Table S7), although several neuron development and differentiation genes were downregulated in *acd* embryos (Table S6). Previously, an important role for p53-dependent apoptosis in neural tube defects and neuronal differentiation was shown in zebrafish (Danilova et al., 2010) and a mouse model, in which *p53* deficiency rescued the neural tube defects (Pani et al., 2002), similar to what we observed in our microarray results. In our analysis, several genes involved in DNA repair, cell cycle, cell division and mitosis were downregulated only in double mutant embryos (Table S8), while genes that promote DNA repair and apoptosis, such as *Ddb2*, *Gadd45b* and *Igfbp3* (insulin-like growth factor binding protein 3), were increased in double mutant embryos (Fig. 5A and data not shown), suggesting p53-independent regulation of cell proliferation by DNA repair mechanisms.

We also observed downregulation of genes functioning in RNA processing, splicing and spliceosome only in double mutant embryos, which might reflect the involvement of RNA splicing in telomere biology (Fig. 5B and Table S8). The direct function of splicing and mRNA-processing factors in DNA damage prevention and repair has been reported (Paulsen et al., 2009; Naro et al., 2015). Consistent with our results, downregulation of splicing factors in response to telomere dysfunction has been reported in a myelodysplastic syndrome (MDS) model (Colla et al., 2015). In addition to the microarray, we showed downregulation of the splicing factors *Prpf19* and *Srsf6* in double mutant embryos with RT-qPCR (Fig. 8A and Fig. 8G). The significant *Prpf19* downregulation in double mutant mice might be particularly important, since in addition to mRNA splicing and spliceosome, *Prpf19* is also involved in DNA damage response and neural differentiation (Urano et al., 2006; Fortschegger et al., 2007; Lu and Legerski, 2007; Song et al., 2010). Deletion of *Prpf19* has been shown to be embryonic lethal in mice (Fortschegger et al., 2007). In human cells and Drosophila, overexpression of *Prpf19* has been shown to extend lifespan by involvement of *Prpf19* in DNA damage (Voglauer et al., 2006; Garschall et al., 2017).

Author Manuscript Author Manuscript Author Manuscript Author Manuscript

Therefore, downregulation of *Prfp19* might be one of the factors contributing to embryonic lethality in double mutant mice although further experimental studies would be needed to confirm this observation.

According to KEGG pathway annotations, some complement and coagulation cascade and apoptosis genes were increased in both *acd* and double mutant embryos (Fig. 6A). It has been shown that when apoptosis is increased, chemotactic factors are released from apoptotic cells to induce mononuclear phagocytes to clear the apoptotic cells (Gregory and Devitt, 2004). In our study, *Elmo3* showed a significant upregulation in both *acd* and double mutant embryos in both microarray and RT-qPCR (Fig. 8C). The significant increase in *Elmo3* expression might be related to clearance of apoptotic cells, since Elmo3 functions in engulfment of apoptotic cells (DeBakker et al., 2004; Kinchen and Ravichandran, 2007). Thus, we speculate that the increased expression of *Elmo3* and other apoptosis genes may represent a clearance mechanism for abnormal cells in both *acd* and double mutant embryos. We also detected upregulated expression of genes that belong to adhesion mechanisms in both in *acd* and double mutant embryos (Fig. 6A). Increased expression of ECM and cell adhesion genes was observed in telomerase deficient ($Terc^{-/-}$) mice, which also exhibit telomere dysfunction (Franco et al., 2005). Increased expression of genes within these pathways may implicate a conserved response to maintain cellular integrity in the presence of abnormal cells.

Several immune system genes were altered in both *acd* and double mutant embryos. We selected *Cxcl14*, which was significantly downregulated in *acd* mutant embryos and upregulated in double mutant embryos, *Irgm1* and *Ifit1*, which were significantly upregulated only in double mutant embryos, and *Usp18*, which was significantly upregulated in both *acd* and double mutant embryos according to our microarray analysis. We observed a similar expression pattern for *Ifit1* and *Usp18* in RT-qPCR (Fig. 8B and Fig. 8D). Expression of *Usp18* might be connected to *Ifit1* expression, since *Usp18* expression was predicted to be regulated by Ifit1 (McDermott et al., 2012).

5. Conclusions

In this study, we investigated the effect of *Acd* and *p53* deficiency in mouse embryos at the transciptome level. Our analyses demonstrate that the majority of differentially expressed genes in *acd* mutant embryos are due to p53-dependent mechanisms and reflect the observed phenotypic differences between *acd* mutant and double mutant embryos. Specifically, several p53 responsive genes and several genes that function in cell cycle, DNA repair, DNA damage and stress response were upregulated in *acd* mutant embryos (Table S5), while several genes involved in transcription, cell cycle, DNA repair, DNA damage and stress response were downregulated in double mutant embryos (Table S8). Our gene expression results for development, morphogenesis and differentiation processes also reflected the phenotypes of *acd* and double mutant embryos. In addition, differentially regulated genes that were independent of p53 included those associated with the immune response, RNA processing and metabolism, DNA repair, and cell cycle. Our results provide novel insights into the molecular basis of the *acd* and double mutant embryo phenotypes and p53-dependent and –independent mechanisms contributing to the *acd* phenotype. In addition to

Author Manuscript Author Manuscript Author Manuscript Author Manuscript

our use of RT-qPCR validations, the effect of the differentially expressed genes on the p53 pathway or on immune response, RNA processing and metabolism, and DNA repair and cell cycle should be verified with additional protein expression studies, including knockdown or overexpression studies, in the future. Given the key role Tpp1 in the shelterin complex and its role in growth, development, and genome stability, our datasets will also be a valuable resource for other investigators studying shelterin function, telomere maintenance and DNA damage responses.

Supplementary Material

Refer to Web version on PubMed Central for supplementary material.

Acknowledgments

We acknowledge Ms. Andrea Krause and Ms. Gail Osawa for technical assistance. We thank Drs. Sally Camper and Jeffrey Innis for critical reading of this manuscript and helpful suggestions.

Funding

This work was funded by NIH grants R01HD058606 and R01AG050509 to CEK. Core support was provided by the MDRTC Cell and Molecular Biology Core NIH grant DK020572 and the UM Comprehensive Cancer Center Core NIH Grant P30CA046592.

List of abbreviations

TPP1	protein encoded by adrenocortical dysplasia gene
Acd	adrenocortical dysplasia gene
acd	adrenocortical dysplasia mutation
p53	transformation related protein 53
DNA	Deoxyribonucleic acid
DC	Dyskeratosis congenita
HHS	Hoyeraal-Hreidarsson syndrome
TRF1	telomere repeat factor-1
TRF2	telomere repeat factor-2
POT1	protection of telomeres-1
RAP1	human homolog of the yeast telomeric protein Rap1
TIN2	tRF1- interacting protein 2
CRS	Caudal Regression syndrome
DW/J	DW/J inbred mouse strain
C57BL6/J	C57BL6/J inbred mouse strain

Author Manuscript Author Manuscript Author Manuscript Author Manuscript

CAST/Ei	CAST/Ei inbred mouse strain
VACTERL	vertebral, anal, cardiac, tracheo-esophageal, renal, limb
RT-qPCR	Quantitative reverse transcription PCR
RNA	Ribonucleic acid
wt	Wild type
GEO	Gene Expression Omnibus
CEL	Affymetrix CEL Data File Format
GO	Gene Ontology
BP	Biological Process
KEGG	Kyoto Encyclopedia of Genes and Genomes
μg	microgram
RIN	RNA integrity number
qPCR	quantitative polymerase chain reaction
cDNA	Complementary DNA
bp	Base pair
UCSC	University of California, Santa Cruz
Δ	Delta
ANOVA	One-way analysis of variance
UTR	untranslated region
RLE	The Relative Log Expression
NUSE	The Normalized Unscaled Standard Error
Prpf19	pre-mRNA processing factor 19
Usp18	ubiquitin specific peptidase 18
Elmo3	engulfment and cell motility 3
Ifit1	interferon-induced protein with tetratricopeptide repeats 1
Irgm1	immunity-related GTPase family M member 1
Cdkn1a	, cyclin-dependent kinase inhibitor 1A (P21)
Srsf6	serine/arginine-rich splicing factor 6
Cxcl14	chemokine (C-X-C motif) ligand 14

Author Manuscript Author Manuscript Author Manuscript Author Manuscript

ECM	extracellular matrix
Tert	telomerase reverse transcriptase
Terc	telomerase RNA component
mRNA	Messenger RNA
Ddb2	damage specific DNA binding protein 2
Gadd45b	growth arrest and DNA-damage-inducible 45 beta
Igfbp3	insulin-like growth factor binding protein 3
MEF	mouse embryonic fibroblasts
Terf2ip	telomeric repeat binding factor 2, interacting protein
Wnt	wingless-type MMTV integration site family
ErbB	epidermal growth factor family of receptor tyrosine kinase
MAPK	mitogen-activated protein kinase
Jak-STAT	Janus kinase/signal transducers and activators of transcription
Fgf3	fibroblast growth factor 3
Fgf4	fibroblast growth factor 4
Fgf13	fibroblast growth factor 13
Fgf10	fibroblast growth factor 10
Jak1	Janus kinase 1
Trp53-	Transformation related protein 53
DDR	DNA damage response
XIAP	X-linked inhibitor of apoptosis
Casp3	Caspase 3
CCL4	chemokine (C-C motif) ligand 4
CCL6	chemokine (C-C motif) ligand 6
CCL8	chemokine (C-C motif) ligand 8
CCL25	chemokine (C-C motif) ligand 25
CXCL14	chemokine (C-X-C motif) ligand 14
CXCL12	chemokine (C-X-C motif) ligand 12
Rad21	RAD21 cohesin complex component

Author Manuscript Author Manuscript Author Manuscript Author Manuscript

Bard1	BRCA1 associated RING domain 1
mTOR	mechanistic target of rapamycin kinase
GnRH	gonadotropin-releasing hormone
VEGF	Vascular endothelial growth factor
Ccnd1	Cyclin D1
DAVID	The Database for Annotation, Visualization and Integrated Discovery
Bbc3	BCL2 binding component 3, also known as Puma
Pten	phosphatase and tensin homolog
Ccng1	cyclin G1

References

Aoude LG, Pritchard AL, Robles-Espinoza CD, Wadt K, Harland M, Choi J, Gartside M, Quesada V, Johansson P, Palmer JM, Ramsay AJ, Zhang X, Jones K, Symmons J, Holland EA, Schmid H, Bonazzi V, Woods S, Dutton-Regester K, Stark MS, Snowden H, van Doorn R, Montgomery GW, Martin NG, Keane TM, Lopez-Otin C, Gerdes AM, Olsson H, Ingvar C, Borg A, Gruis NA, Trent JM, Jonsson G, Bishop DT, Mann GJ, Newton-Bishop JA, Brown KM, Adams DJ and Hayward NK, 2015 Nonsense mutations in the shelterin complex genes ACD and TERF2IP in familial melanoma. J Natl Cancer Inst 107.

Baumann P and Cech TR, 2001 Pot1, the putative telomere end-binding protein in fission yeast and humans. Science 292, 1171–5. [PubMed: 11349150]

Beamer WG, Sweet HO, Bronson RT, Shire JG, Orth DN and Davisson MT, 1994 Adrenocortical dysplasia: a mouse model system for adrenocortical insufficiency. J Endocrinol 141, 33–43. [PubMed: 8014601]

Bolstad BM CF, Brettschneider J, Simpson K, Cope L, Irizarry RA, Speed TP, 2005 Quality assessment of affymetrix GeneChip data In: Bioinformatics and Computational Biology Solutions Using R and Bioconductor. Gentleman R, Carey, Huber W, Irizarry R and Dudoit S (eds.). Springer, New York,, 33–47.

Broccoli D, Smogorzewska A, Chong L and de Lange T, 1997 Human telomeres contain two distinct Mybrelated proteins, TRF1 and TRF2. Nat Genet 17, 231–5. [PubMed: 9326950]

Brogna S and Wen J, 2009 Nonsense-mediated mRNA decay (NMD) mechanisms. Nat Struct Mol Biol 16, 107–13. [PubMed: 19190664]

Casimiro MC, Crosariol M, Loro E, Li Z and Pestell RG, 2012 Cyclins and cell cycle control in cancer and disease. Genes Cancer 3, 649–57. [PubMed: 23634253]

Celli GB and de Lange T, 2005 DNA processing is not required for ATM-mediated telomere damage response after TRF2 deletion. Nat Cell Biol 7, 712–8. [PubMed: 15968270]

Chiang YJ, Kim SH, Tessarollo L, Campisi J and Hodes RJ, 2004 Telomere-associated protein TIN2 is essential for early embryonic development through a telomerase-independent pathway. Molecular and Cellular Biology 24, 6631–6634. [PubMed: 15254230]

Colla S, Ong DS, Ogoti Y, Marchesini M, Mistry NA, Clise-Dwyer K, Ang SA, Storti P, Viale A, Giuliani N, Ruisaard K, Ganan Gomez I, Bristow CA, Estecio M, Weksberg DC, Ho YW, Hu B, Genovese G, Pettazzoni P, Multani AS, Jiang S, Hua S, Ryan MC, Carugo A, Nezi L, Wei Y, Yang H, D'Anca M, Zhang L, Gaddis S, Gong T, Horner JW, Heffernan TP, Jones P, Cooper LJ, Liang H, Kantarjian H, Wang YA, Chin L, Bueso-Ramos C, Garcia-Manero G and DePinho RA, 2015 Telomere dysfunction drives aberrant hematopoietic differentiation and myelodysplastic syndrome. Cancer Cell 27, 644–57. [PubMed: 25965571]

Author Manuscript Author Manuscript Author Manuscript Author Manuscript

Danilova N, Kumagai A and Lin J, 2010 p53 upregulation is a frequent response to deficiency of cell-essential genes. PLoS One 5, e15938. [PubMed: 21209837]

de Hoon MJL, Imoto S, Nolan J and Miyano S, 2004 Open source clustering software. Bioinformatics 20, 1453–1454. [PubMed: 14871861]

DeBakker CD, Haney LB, Kinchen JM, Grimsley C, Lu MJ, Klingele D, Hsu PK, Chou BK, Cheng LC, Blangy A, Sondek J, Hengartner MO, Wu YC and Ravichandran KS, 2004 Phagocytosis of apoptotic cells is regulated by a UNC-73/TRIO-MIG-2/RhoG signaling module and armadillo repeats of CED-12/ELMO. Current Biology 14, 2208–2216. [PubMed: 15620647]

Dorey K and Amaya E, 2010 FGF signalling: diverse roles during early vertebrate embryogenesis. Development 137, 3731–42. [PubMed: 20978071]

Eisen MB, Spellman PT, Brown PO and Botstein D, 1998 Cluster analysis and display of genome-wide expression patterns. Proceedings of the National Academy of Sciences of the United States of America 95, 14863–14868. [PubMed: 9843981]

Else T, Theisen BK, Wu Y, Hutz JE, Keegan CE, Hammer GD and Ferguson DO, 2007 Tpp1/Acd maintains genomic stability through a complex role in telomere protection. Chromosome Res 15, 1001–13. [PubMed: 18185984]

Else T, Trovato A, Kim AC, Wu Y, Ferguson DO, Kuick RD, Lucas PC and Hammer GD, 2009 Genetic p53 deficiency partially rescues the adrenocortical dysplasia phenotype at the expense of increased tumorigenesis. Cancer Cell 15, 465–76. [PubMed: 19477426]

Fortschegger K, Wagner B, Voglauer R, Katinger H, Sibilia M and Grillari J, 2007 Early embryonic lethality of mice lacking the essential protein SNEV. Mol Cell Biol 27, 3123–30. [PubMed: 17283042]

Franco S, Canela A, Klatt P and Blasco MA, 2005 Effectors of mammalian telomere dysfunction: a comparative transcriptome analysis using mouse models. Carcinogenesis 26, 1613–26. [PubMed: 15860505]

Garschall K, Dellago H, Galikova M, Schosserer M, Flatt T and Grillari J, 2017 Ubiquitous overexpression of the DNA repair factor dPrp19 reduces DNA damage and extends Drosophila life span. NPJ Aging Mech Dis 3, 5. [PubMed: 28649423]

Gautier L, Cope L, Bolstad BM and Irizarry RA, 2004 affy--analysis of Affymetrix GeneChip data at the probe level. Bioinformatics 20, 307–15. [PubMed: 14960456]

Gregory CD and Devitt A, 2004 The macrophage and the apoptotic cell: an innate immune interaction viewed simplistically? Immunology 113, 1–14.

Guieze R, Pages M, Veronese L, Combes P, Lemal R, Gay-Bellile M, Chauvet M, Callanan M, Kwiatkowski F, Pereira B, Vago P, Bay JO, Tournilhac O and Tchirkov A, 2016 Telomere status in chronic lymphocytic leukemia with TP53 disruption. Oncotarget 7, 56976–56985. [PubMed: 27486974]

Guo X, Deng Y, Lin Y, Cosme-Blanco W, Chan S, He H, Yuan G, Brown EJ and Chang S, 2007 Dysfunctional telomeres activate an ATM-ATR-dependent DNA damage response to suppress tumorigenesis. EMBO J 26, 4709–19. [PubMed: 17948054]

Hockemeyer D, Daniels JP, Takai H and de Lange T, 2006 Recent expansion of the telomeric complex in rodents: Two distinct POT1 proteins protect mouse telomeres. Cell 126, 63–77. [PubMed: 16839877]

Hockemeyer D, Palm W, Else T, Daniels JP, Takai KK, Ye JZ, Keegan CE, de Lange T and Hammer GD, 2007 Telomere protection by mammalian Pot1 requires interaction with Tpp1. Nat Struct Mol Biol 14, 754–61. [PubMed: 17632522]

Hoffmeyer K, Raggioli A, Rudloff S, Anton R, Hierholzer A, Del Valle I, Hein K, Vogt R and Kemler R, 2012 Wnt/beta-catenin signaling regulates telomerase in stem cells and cancer cells. Science 336, 1549–54. [PubMed: 22723415]

Houghtaling BR, Cuttonaro L, Chang W and Smith S, 2004 A dynamic molecular link between the telomere length regulator TRF1 and the chromosome end protector TRF2. Current Biology 14, 1621–1631. [PubMed: 15380063]

Huang da W, Sherman BT and Lempicki RA, 2009a Bioinformatics enrichment tools: paths toward the comprehensive functional analysis of large gene lists. Nucleic Acids Res 37, 1–13. [PubMed: 19033363]

Author Manuscript Author Manuscript Author Manuscript Author Manuscript

Huang da W, Sherman BT and Lempicki RA, 2009b Systematic and integrative analysis of large gene lists using DAVID bioinformatics resources. Nat Protoc 4, 44–57. [PubMed: 19131956]

Jacks T, Remington L, Williams BO, Schmitt EM, Halachmi S, Bronson RT and Weinberg RA, 1994 Tumor spectrum analysis in p53-mutant mice. Curr Biol 4, 1–7. [PubMed: 7922305]

Jones M, Bisht K, Savage SA, Nandakumar J, Keegan CE and Maillard I, 2016 The shelterin complex and hematopoiesis. J Clin Invest 126, 1621–9. [PubMed: 27135879]

Jones M, Osawa G, Regal JA, Weinberg DN, Taggart J, Kocak H, Friedman A, Ferguson DO, Keegan CE and Maillard I, 2014 Hematopoietic stem cells are acutely sensitive to Acd shelterin gene inactivation. J Clin Invest 124, 353–66. [PubMed: 24316971]

Karlseder J, Broccoli D, Dai Y, Hardy S and de Lange T, 1999 p53- and ATM-dependent apoptosis induced by telomeres lacking TRF2. Science 283, 1321–5. [PubMed: 10037601]

Karlseder J, Kachatrian L, Takai H, Mercer K, Hingorani S, Jacks T and de Lange T, 2003 Targeted deletion reveals an essential function for the telomere length regulator Trf1. Mol Cell Biol 23, 6533–41. [PubMed: 12944479]

Keegan CE, Hutz JE, Else T, Adamska M, Shah SP, Kent AE, Howes JM, Beamer WG and Hammer GD, 2005 Urogenital and caudal dysgenesis in adrenocortical dysplasia (acd) mice is caused by a splicing mutation in a novel telomeric regulator. Hum Mol Genet 14, 113–23. [PubMed: 15537664]

Kibe T, Osawa GA, Keegan CE and de Lange T, 2010 Telomere protection by TPP1 is mediated by POT1a and POT1b. Mol Cell Biol 30, 1059–66. [PubMed: 19995905]

Kimura SH, Ikawa M, Ito A, Okabe M and Nojima H, 2001 Cyclin G1 is involved in G2/M arrest in response to DNA damage and in growth control after damage recovery. Oncogene 20, 3290–300. [PubMed: 11423978]

Kinchen JM and Ravichandran KS, 2007 Journey to the grave: signaling events regulating removal of apoptotic cells. J Cell Sci 120, 2143–9. [PubMed: 17591687]

Kocak H, Ballew BJ, Bisht K, Eggebeen R, Hicks BD, Suman S, O'Neil A, Giri N, Laboratory NDCGR, Group NDCSW, Maillard I, Alter BP, Keegan CE, Nandakumar J and Savage SA, 2014 Hoyeraal-Hreidarsson syndrome caused by a germline mutation in the TEL patch of the telomere protein TPP1. Genes Dev 28, 2090–102. [PubMed: 25233904]

Kuhlow D, Florian S, von Figura G, Weimer S, Schulz N, Petzke KJ, Zarse K, Pfeiffer AF, Rudolph KL and Ristow M, 2010 Telomerase deficiency impairs glucose metabolism and insulin secretion. Aging (Albany NY) 2, 650–8. [PubMed: 20876939]

Latrick CM and Cech TR, 2010 POT1-TPP1 enhances telomerase processivity by slowing primer dissociation and aiding translocation. EMBO J 29, 924–33. [PubMed: 20094033]

Li B and de Lange T, 2003 Rap1 affects the length and heterogeneity of human telomeres. Mol Biol Cell 14, 5060–8. [PubMed: 14565979]

Li Z, Jiao X, Wang C, Shirley LA, Elsaleh H, Dahl O, Wang M, Soutoglou E, Knudsen ES and Pestell RG, 2010 Alternative cyclin D1 splice forms differentially regulate the DNA damage response. Cancer Res 70, 8802–11. [PubMed: 20940395]

Liu D, O'Connor MS, Qin J and Songyang Z, 2004 Telosome, a mammalian telomere-associated complex formed by multiple telomeric proteins. J Biol Chem 279, 51338–42. [PubMed: 15383534]

Livak KJ and Schmittgen TD, 2001 Analysis of relative gene expression data using real-time quantitative PCR and the 2(-Delta Delta C(T)) Method. Methods 25, 402–8. [PubMed: 11846609]

Lu X and Legerski RJ, 2007 The Prp19/Pso4 core complex undergoes ubiquitylation and structural alterations in response to DNA damage. Biochem Biophys Res Commun 354, 968–74. [PubMed: 17276391]

Martinez P, Thanasoula M, Carlos AR, Gomez-Lopez G, Tejera AM, Schoeftner S, Dominguez O, Pisano DG, Tarsounas M and Blasco MA, 2010 Mammalian Rap1 controls telomere function and gene expression through binding to telomeric and extratelomeric sites. Nat Cell Biol 12, 768–80. [PubMed: 20622869]

McDermott JE, Vartanian KB, Mitchell H, Stevens SL, Sanfilippo A and Stenzel-Poore MP, 2012 Identification and validation of Ifit1 as an important innate immune bottleneck. PLoS One 7, e36465. [PubMed: 22745654]

Author Manuscript Author Manuscript Author Manuscript Author Manuscript

Nakano K and Vousden KH, 2001 PUMA, a novel proapoptotic gene, is induced by p53. Mol Cell 7, 683–94. [PubMed: 11463392]

Nakashima M, Nandakumar J, Sullivan KD, Espinosa JM and Cech TR, 2013 Inhibition of telomerase recruitment and cancer cell death. J Biol Chem 288, 33171–80. [PubMed: 24097987]

Naro C, Bielli P, Pagliarini V and Sette C, 2015 The interplay between DNA damage response and RNA processing: the unexpected role of splicing factors as gatekeepers of genome stability. Front Genet 6, 142. [PubMed: 25926848]

O'Connor MS, Safari A, Liu D, Qin J and Songyang Z, 2004 The human Rap1 protein complex and modulation of telomere length. J Biol Chem 279, 28585–91. [PubMed: 15100233]

Palm W and de Lange T, 2008 How Shelterin Protects Mammalian Telomeres. Annual Review of Genetics 42, 301–334.

Pani L, Horal M and Loeken MR, 2002 Rescue of neural tube defects in Pax-3-deficient embryos by p53 loss of function: implications for Pax-3- dependent development and tumorigenesis. Genes Dev 16, 676–80. [PubMed: 11914272]

Park JI, Venteicher AS, Hong JY, Choi J, Jun S, Shkreli M, Chang W, Meng Z, Cheung P, Ji H, McLaughlin M, Veenstra TD, Nusse R, McCrea PD and Artandi SE, 2009 Telomerase modulates Wnt signalling by association with target gene chromatin. Nature 460, 66–72. [PubMed: 19571879]

Paulsen RD, Soni DV, Wollman R, Hahn AT, Yee MC, Guan A, Hesley JA, Miller SC, Cromwell EF, Solow-Cordero DE, Meyer T and Cimprich KA, 2009 A genome-wide siRNA screen reveals diverse cellular processes and pathways that mediate genome stability. Mol Cell 35, 228–39. [PubMed: 19647519]

Sahin E, Colla S, Liesa M, Moslehi J, Muller FL, Guo M, Cooper M, Kotton D, Fabian AJ, Walkey C, Maser RS, Tonon G, Foerster F, Xiong R, Wang YA, Shukla SA, Jaskelioff M, Martin ES, Heffernan TP, Protopopov A, Ivanova E, Mahoney JE, Kost-Alimova M, Perry SR, Bronson R, Liao R, Mulligan R, Shirihai OS, Chin L and DePinho RA, 2011 Telomere dysfunction induces metabolic and mitochondrial compromise. Nature 470, 359–65. [PubMed: 21307849]

Saldanha AJ, 2004 Java Treeview-extensible visualization of microarray data. Bioinformatics 20, 3246–3248. [PubMed: 15180930]

Samassekou O, Bastien N, Lichtensztejn D, Yan J, Mai S and Drouin R, 2014 Different TP53 mutations are associated with specific chromosomal rearrangements, telomere length changes, and remodeling of the nuclear architecture of telomeres. Genes Chromosomes Cancer 53, 934–50. [PubMed: 25059482]

Savage SA, Giri N, Baerlocher GM, Orr N, Lansdorp PM and Alter BP, 2008 TINF2, a component of the shelterin telomere protection complex, is mutated in dyskeratosis congenita. Am J Hum Genet 82, 501–9. [PubMed: 18252230]

Sfeir A and de Lange T, 2012 Removal of shelterin reveals the telomere end-protection problem. Science 336, 593–7. [PubMed: 22556254]

Sfeir A, Kosiyatrakul ST, Hockemeyer D, MacRae SL, Karlseder J, Schildkraut CL and de Lange T, 2009 Mammalian telomeres resemble fragile sites and require TRF1 for efficient replication. Cell 138, 90–103. [PubMed: 19596237]

Smogorzewska A, van Steensel B, Bianchi A, Oelmann S, Schaefer MR, Schnapp G and de Lange T, 2000 Control of human telomere length by TRF1 and TRF2. Mol Cell Biol 20, 1659–68. [PubMed: 10669743]

Song EJ, Werner SL, Neubauer J, Stegmeier F, Aspden J, Rio D, Harper JW, Elledge SJ, Kirschner MW and Rape M, 2010 The Prp19 complex and the Usp4(Sart3) deubiquitinating enzyme control reversible ubiquitination at the spliceosome. Genes & Development 24, 1434–1447. [PubMed: 20595234]

Stambolic V, MacPherson D, Sas D, Lin Y, Snow B, Jang Y, Benchimol S and Mak TW, 2001 Regulation of PTEN transcription by p53. Mol Cell 8, 317–25. [PubMed: 11545734]

Takai KK, Kibe T, Donigian JR, Frescas D and de Lange T, 2011 Telomere protection by TPP1/POT1 requires tethering to TIN2. Mol Cell 44, 647–59. [PubMed: 22099311]

Tan T and Chu G, 2002 p53 Binds and activates the xeroderma pigmentosum DDB2 gene in humans but not mice. Mol Cell Biol 22, 3247–54. [PubMed: 11971958]

Author Manuscript Author Manuscript Author Manuscript Author Manuscript

Urano Y, Iiduka M, Sugiyama A, Akiyama H, Uzawa K, Matsumoto G, Kawasaki Y and Tashiro F, 2006 Involvement of the mouse Prp19 gene in neuronal/astroglial cell fate decisions. J Biol Chem 281, 7498–514. [PubMed: 16352598]

Vairapandi M, Balliet AG, Fornace AJ, Jr., Hoffman B and Liebermann DA, 1996 The differentiation primary response gene MyD118, related to GADD45, encodes for a nuclear protein which interacts with PCNA and p21WAF1/CIP1. Oncogene 12, 2579–94. [PubMed: 8700517]

Vlangos CN, O'Connor BC, Morley MJ, Krause AS, Osawa GA and Keegan CE, 2009 Caudal regression in adrenocortical dysplasia (acd) mice is caused by telomere dysfunction with subsequent p53-dependent apoptosis. Dev Biol 334, 418–28. [PubMed: 19660449]

Voglauer R, Chang MW, Dampier B, Wieser M, Baumann K, Sterovsky T, Schreiber M, Katinger H and Grillari J, 2006 SNEV overexpression extends the life span of human endothelial cells. Exp Cell Res 312, 746–59. [PubMed: 16388800]

Walne AJ, Vulliamy T, Beswick R, Kirwan M and Dokal I, 2008 TINF2 mutations result in very short telomeres: analysis of a large cohort of patients with dyskeratosis congenita and related bone marrow failure syndromes. Blood 112, 3594–600. [PubMed: 18669893]

Wang F, Podell ER, Zaug AJ, Yang YT, Baciu P, Cech TR and Lei M, 2007 The POT1-TPP1 telomere complex is a telomerase processivity factor. Nature 445, 506–510. [PubMed: 17237768]

Woo M, Hakem A, Elia AJ, Hakem R, Duncan GS, Patterson BJ and Mak TW, 1999 In vivo evidence that caspase-3 is required for Fas-mediated apoptosis of hepatocytes. J Immunol 163, 4909–16. [PubMed: 10528193]

Wu L, Multani AS, He H, Cosme-Blanco W, Deng Y, Deng JM, Bachilo O, Pathak S, Tahara H, Bailey SM, Deng Y, Behringer RR and Chang S, 2006 Pot1 deficiency initiates DNA damage checkpoint activation and aberrant homologous recombination at telomeres. Cell 126, 49–62. [PubMed: 16839876]

Xin H, Liu D, Wan M, Safari A, Kim H, Sun W, O'Connor MS and Songyang Z, 2007 TPP1 is a homologue of ciliate TEBP-beta and interacts with POT1 to recruit telomerase. Nature 445, 559–62. [PubMed: 17237767]

Ye JZ, Donigian JR, van Overbeek M, Loayza D, Luo Y, Krutchinsky AN, Chait BT and de Lange T, 2004 TIN2 binds TRF1 and TRF2 simultaneously and stabilizes the TRF2 complex on telomeres. J Biol Chem 279, 47264–71. [PubMed: 15316005]

Author Manuscript Author Manuscript Author Manuscript Author Manuscript

Highlights

- Most differentially expressed genes in *acd* mutant embryos are p53-dependent
- Genes in cell cycle and DNA repair are differentially expressed in *acd* embryos
- Differentially expressed pathways correlate with phenotypes of *acd* mutant embryos
- Some immune response genes are differentially expressed independently of p53
- Some RNA processing genes are differentially expressed independently of p53

Author Manuscript Author Manuscript Author Manuscript Author Manuscript

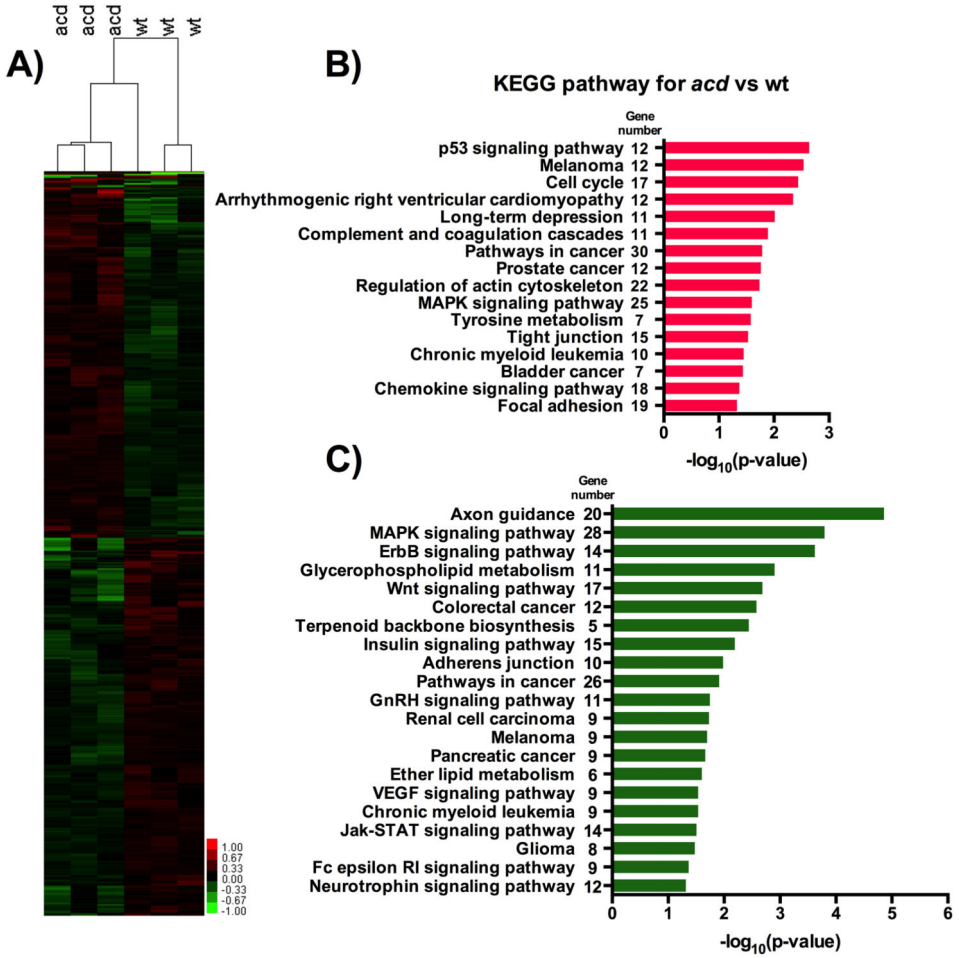

Fig. 1.

(A) Heat-map of differentially expressed probe sets in *acd* embryos (n=3) when compared to wt embryos (n=3). (B) KEGG pathway annotation of upregulated genes in *acd* embryos. (C) KEGG pathway annotation of downregulated genes in *acd* embryos. (B-C) Gene counts for each pathway term is provided. Each bar indicates the significance of the related pathway term. Red coloring indicates upregulation, while green coloring indicates downregulation of probe sets in the *acd* embryos (*acd* vs. wt).

Author Manuscript Author Manuscript Author Manuscript Author Manuscript

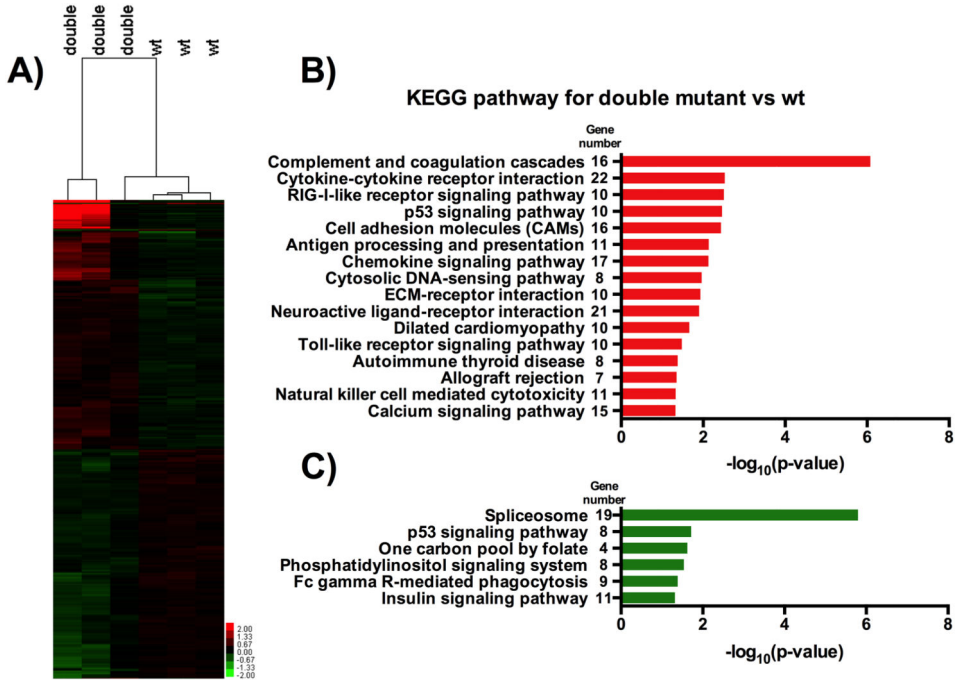

Fig. 2.

(A) Heat-map of differentially expressed probe sets in double mutant embryos (n=3) when compared to wt embryos (n=3). (B) KEGG pathway annotation of upregulated genes in double mutant embryos. (C) KEGG pathway annotation of downregulated genes in double mutant embryos. (B-C) Gene counts for each pathway term is provided. Each bar indicates the significance of the related pathway term. Red coloring indicates upregulation, while green coloring indicates downregulation of probe sets in the double mutant embryos (double vs. wt).

Author Manuscript Author Manuscript Author Manuscript Author Manuscript

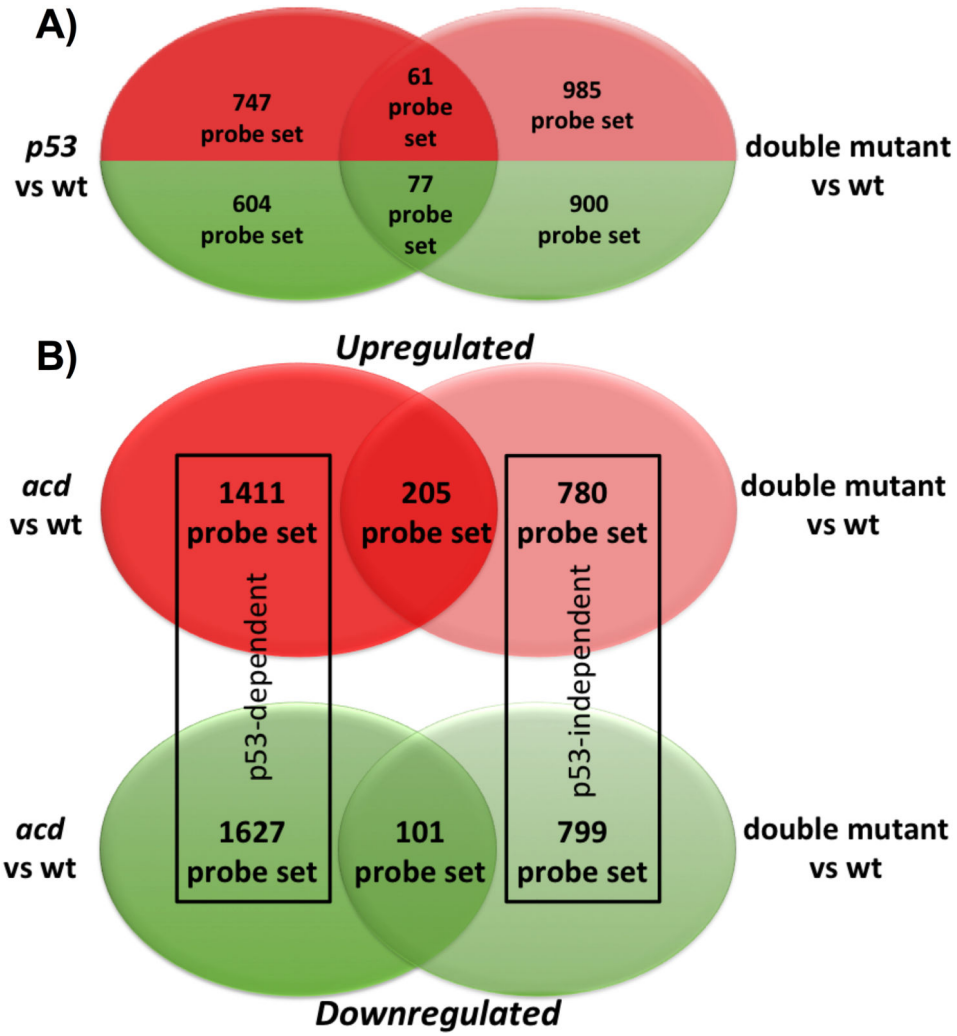

Fig. 3.

(A) Venn diagram of differentially expressed probe sets that are shared or specific to *p53* (*p53* vs. wt) and double mutant embryos (double vs. wt) (B) Venn diagram of differentially expressed probe sets that are *p53*dependent or –independent according to *acd* and double mutant (after *p53* shared probe sets were excluded) comparison. Red coloring (upper parts) of the venn diagrams indicates upregulated probe sets and green coloring (below parts) of the venn diagrams indicates downregulated probe sets.

Author Manuscript Author Manuscript Author Manuscript Author Manuscript

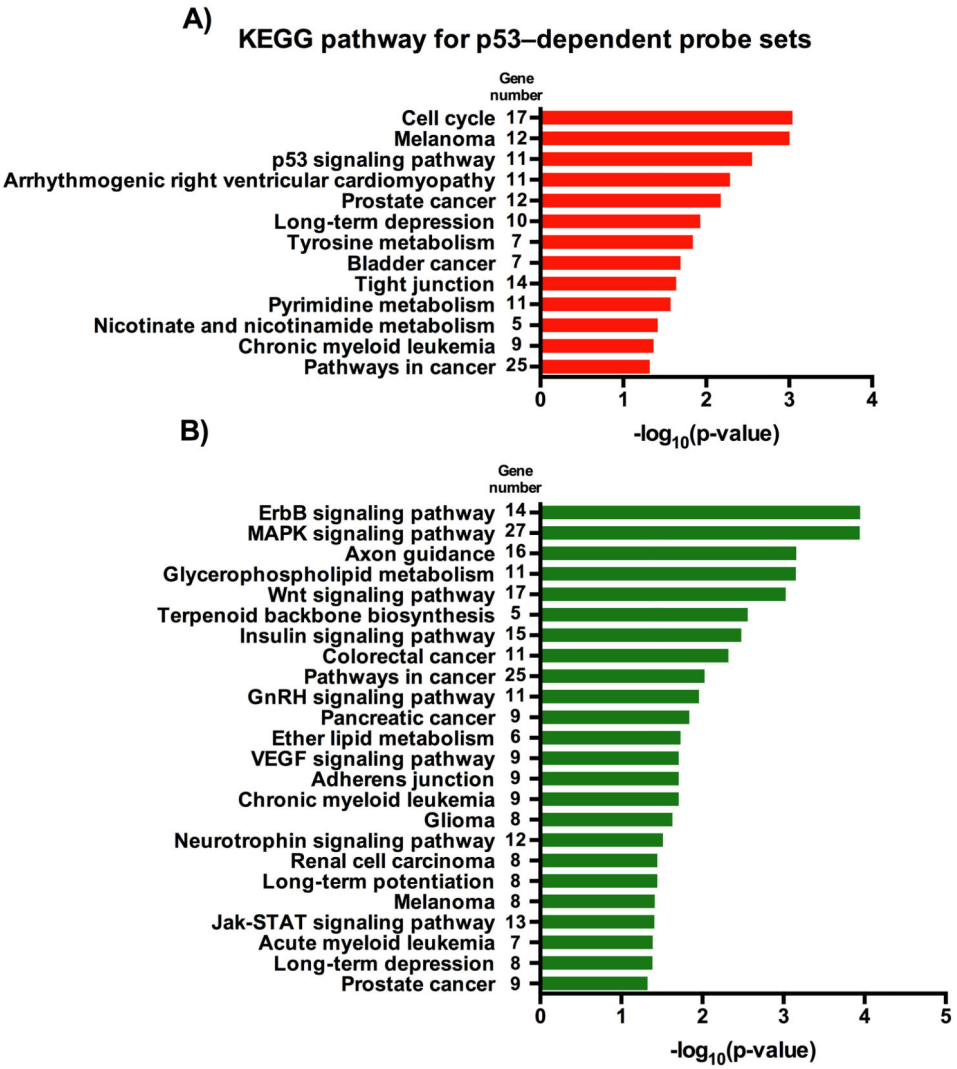

Fig. 4.

KEGG pathway annotation of p53–dependent (A) upregulated (red colored bars) and (B) downregulated (green colored bars) probe sets involved in the *acd* phenotype. Gene counts for each pathway term is provided. Each bar indicates the significance of the related pathway term.

Author Manuscript Author Manuscript Author Manuscript Author Manuscript

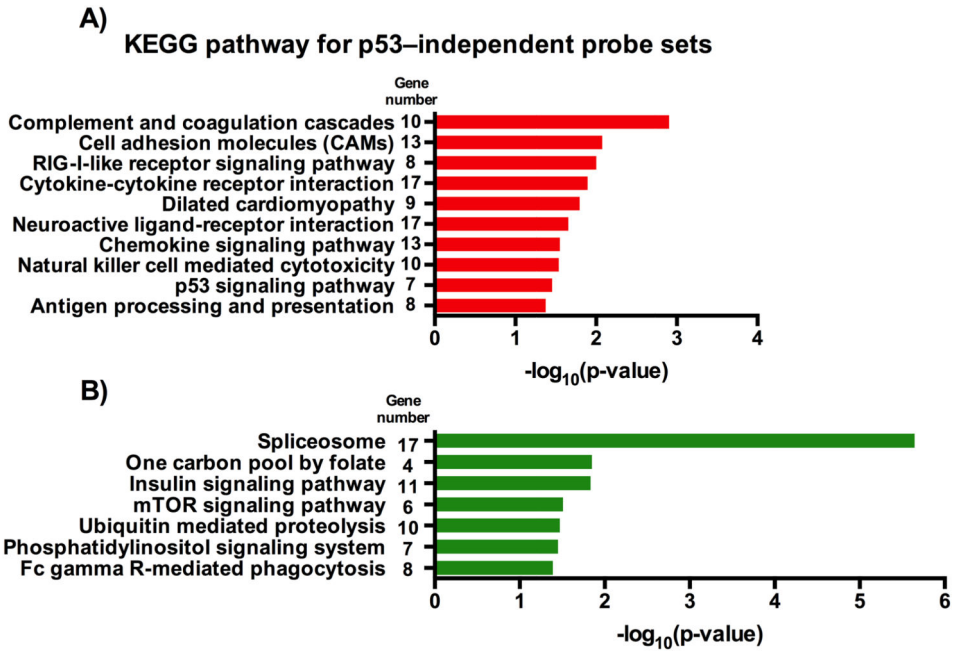

Fig. 5.

KEGG pathway annotation of p53–independent (A) upregulated (red colored bars) and (B) downregulated (green colored bars) probe sets involved in the *acd* phenotype. Gene counts for each pathway term is provided. Each bar indicates the significance of the related pathway term.

Author Manuscript Author Manuscript Author Manuscript Author Manuscript

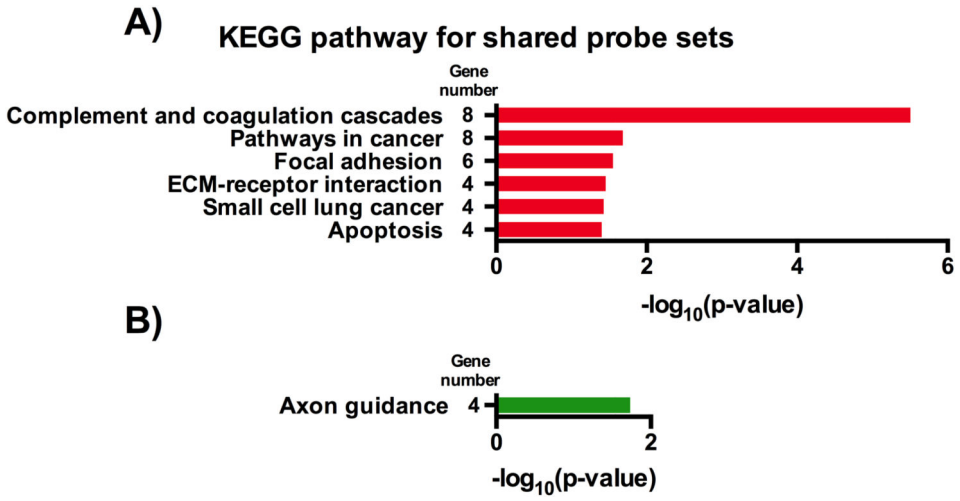

Fig. 6.

KEGG pathway annotation of (A) upregulated (red colored bars) and (B) downregulated (green colored bars) probe sets that were shared between *acd* and double mutant embryos. Gene counts for each pathway term is provided. Each bar indicates the significance of the related pathway term.

Author Manuscript Author Manuscript Author Manuscript Author Manuscript

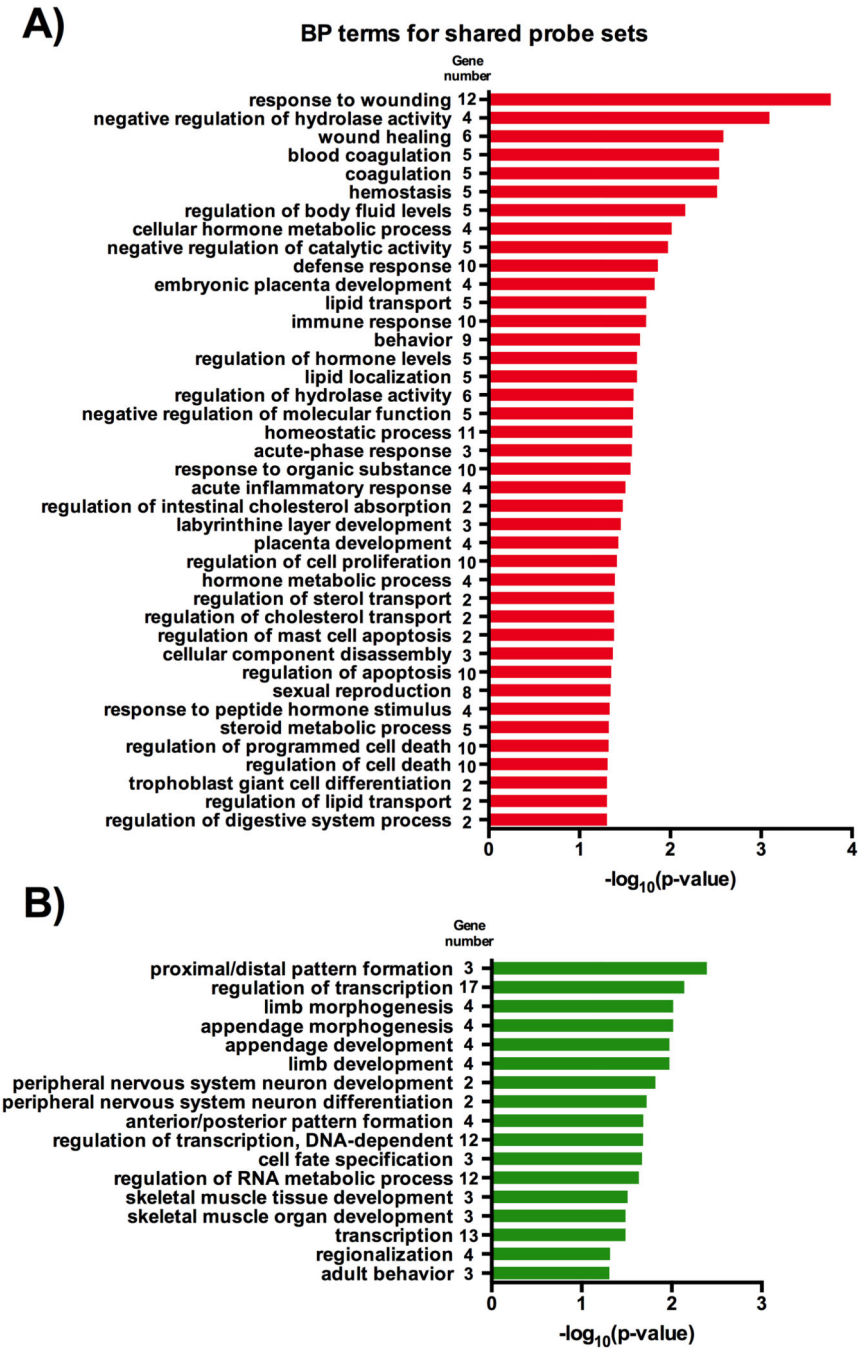

Fig. 7.

GO for Biological Process (BP) term annotation of (A) upregulated (red colored bars) and (B) downregulated (green colored bars) probe sets that were shared between *acd* and double mutant embryos. Gene counts for each BP term is provided. Each bar indicates the significance of the related BP term.

Author Manuscript
Author Manuscript
Author Manuscript
Author Manuscript

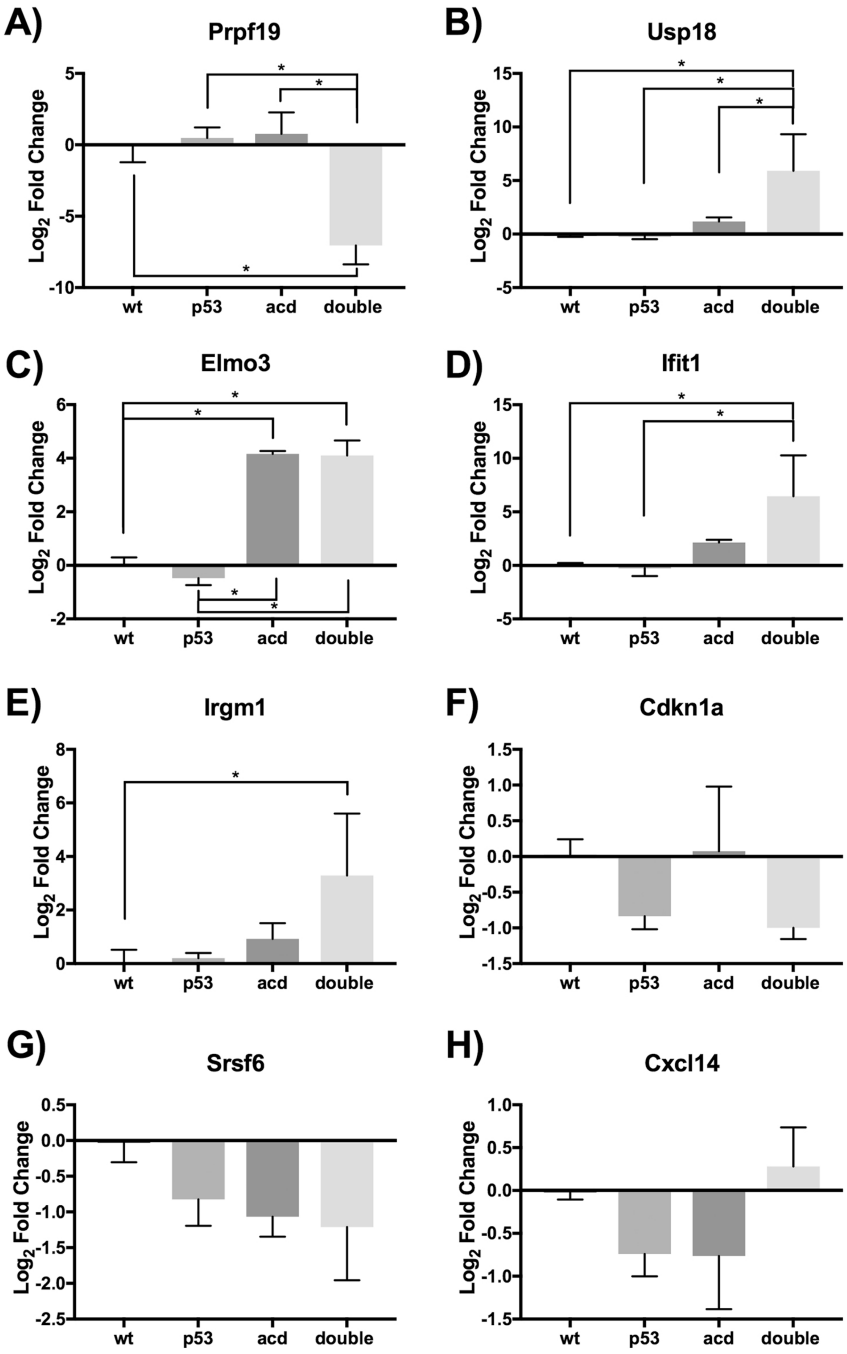

Fig. 8.

The significantly altered genes in microarray analysis that were selected for RT-qPCR validation, (A) *Prpf19*, (B) *Usp18*, (C) *Elmo3*, (D) *Ifit1*, (E) *Irgm1*, (F) *Cdkn1a*, (G) *Srsf6*, (H) *Cxcl14*. One-way ANOVA with Tukey multiple comparison test, *Prpf19*, Pwt vs. double<0.001, Pp53 vs. double<0.001, Pacd vs. double<0.001; *Usp18*, Pwt vs. double=0.013, Pp53 vs. double=0.011, Pacd vs. double=0.04; *Elmo3*, Pwt vs. acd<0.001, Pwt vs. double<0.001, Pp53 vs. acd<0.001, Pp53 vs. double<0.001; *Ifit1*, $P_{wt\ vs.\ double}$=0.016, $P_{p53\ vs.\ double}$=0.013; *Irgm1*, $P_{wt\ vs.\ double}$=0.044. * indicates statistically

Author Manuscript Author Manuscript Author Manuscript Author Manuscript

significant differences (P<0.05) between groups. *Prpf19* (pre-mRNA processing factor 19), *Usp18* (ubiquitin specific peptidase 18), *Elmo3* (engulfment and cell motility 3), *Ifit1* (interferon-induced protein with tetratricopeptide repeats 1), *Irgm1* (immunityrelated GTPase family M member 1), *Cdkn1a* (cyclin-dependent kinase inhibitor 1A (P21)), *Srsf6* (serine/arginineric splicing factor 6), *Cxcl14* (chemokine (C-X-C motif) ligand 14).